Fundamental Studies of Microscopic Wetting on Organic Surfaces. 2. Interaction of Secondary Adsorbates with Chemically Textured Organic Monolayers[1]

Lawrence H. Dubois,* Bernard R. Zegarski, and Ralph G. Nuzzo*

Contribution from the AT&T Bell Laboratories, Murray Hill, New Jersey 07974.
Received February 17, 1989

Abstract: Self-assembled monolayers of a series of terminally substituted alkyl thiols and disulfides chemisorbed on an Au(111) single-crystal surface were used as substrates for subsequent temperature-programmed desorption (TPD) studies. The monolayers studied were derived from adsorbates of the general structure $HS(CH_2)_{15}X$ or $(S(CH_2)_{15}X)_2$ (where X = CH_3, CO_2CH_3, CH_2OH, CO_2H, and $CONH_2$). The adsorption of *n*-hexane, methanol, and water on these materials as well as on the clean Au(111) surface was examined. The data reveal complex behavior for the adsorption of secondary overlayers on these dense molecular solids especially in those substrate–adsorbate pairings capable of forming interlayer hydrogen bonds. It is also found that certain correlations can be made between the TPD data, a microscopic measurement, and the macroscopic wetting properties as defined by contact angle data.

Most of what we know about the properties of "solid" organic surfaces has been obtained through the application of a very simple experimental procedure, the measurement of contact angles.[2] The literature describes many different implementations of this technique. The simplest and perhaps most representative form of this measurement is illustrated in Scheme I. The characteristic actually measured in such an experiment is the angle, θ, formed by a drop of a probe liquid contacting a surface under study. There are many protocols one can use to interpret such data.[2] At the heart of most is the description of a potentially complex three-phase equilibrium in terms of simple thermodynamic arguments. The earliest such treatment was given by Young (eq 1) in which

$$\gamma_{sv} - \gamma_{sl} = \gamma_{lv} \cos \theta \qquad (1)$$

the angle, θ, is described explicitly in terms of the three relevant interfacial tensions (see Scheme I). This equation describes, in an ideal case, the surface free energy of a solid. It is also clear from the data now available that this measurement possesses extreme surface sensitivity, responding to molecular structure within the topmost few angstroms of a solid.[3] There is, however, a limitation intrinsic to contact angle measurements which has tended to greatly diminish their utility, namely that they contain relatively little information. What we observe in contact angle behavior is a macroscopic property of the system. There is little direct connection made with or inferred about the underlying microscopic characteristics of the surface in question. This type of experiment is also very sensitive to artifacts and complications arising from such features of real surfaces as compositional heterogeneity and roughness.[2-5]

Our interest in the current work is in studying the structural basis of important surface phenomena of organic materials. Our approach has been 2-fold. First, we have attempted to prepare model organic substrates with well-defined structural characteristics amenable to further detailed study. Second, we have sought to apply modern surface spectroscopies to the problem of interfacial properties in the hope of elaborating a detailed microscopic understanding complementary to that being developed by others with the more macroscopic measure of wetting.[3-5] The first paper in this series described the synthetic and structural aspects of this program.[1] The structurally self-consistent series of substituted alkanethiol monolayers on gold described in that study and accompanying references provides the starting point for this paper. In the present report, we describe how we have used these unique structures to measure the adsorption properties of organic surfaces at the microscopic level. Our experimental method is depicted schematically. As is shown in Scheme II, we have examined the adsorption of secondary adsorbates on top of these model substrates. In order to effect control over the coverage of the molecules in the adsorbed overlayer, these experiments were conducted in an ultrahigh vacuum (UHV) environment. Various adsorbates were used, including hydrogen-bonding systems such as water and methanol. Coverages of the overlayer were varied widely—from fractions of a monolayer to thick multilayers. The nature and strengths of the interactions between various adsorbate–substrate pairings were then determined by using temper-

Scheme I

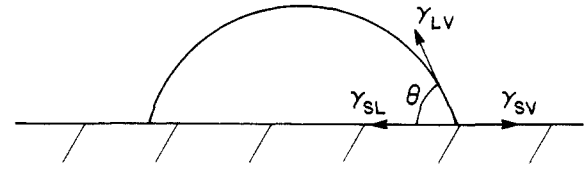

Scheme II

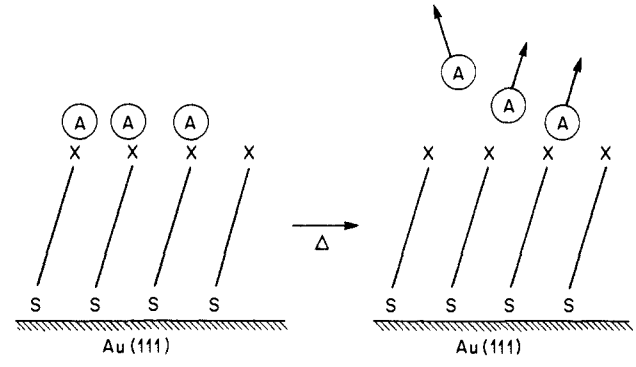

[a] S-X ≡ $HS(CH_2)_{15}X$: X = CH_3, CO_2CH_3, CH_2OH, $CONH_2$, CO_2H; A = H_2O, CH_3OH, *n*-C_6H_{14}.

(1) Nuzzo, R. G.; Dubois, L. H.; Allara, D. L. *J. Am. Chem. Soc.*, preceding paper in this issue.

(2) See, for example, the relevant discussion in Kaelbe, D. H. *Physical Chemistry of Adhesion*; Wiley Interscience: New York, 1971. *Contact Angle: Wettability and Adhesion*; ACS Advances in Chemistry Series 43; American Chemical Society: Washington, DC, 1964. Adamson, A. W. *Physical Chemistry of Surfaces*; J. Wiley: New York, 1982. *Surface and Colloid Science*; Good, R. J., Stromberg, R. R., Eds.; Plenum Press: New York, 1979; Vol. 11 and references cited therein.

(3) Bain, C. D.; Whitesides, G. M. *J. Am. Chem. Soc.* **1988**, *110*, 5897-5898. Bain, C. D.; Whitesides, G. M. *J. Am. Chem. Soc.* **1988**, *110*, 3665-3666 and references cited therein.

(4) Bain, C. D.; Whitesides, G. M. *J. Am. Chem. Soc.* **1989**, *111*, 7164-7175.

(5) Bain, C. D.; Whitesides, G. M. *J. Am. Chem. Soc.* **1988**, *110*, 6560-6561.

0002-7863/90/1512-570$02.50/0

ature-programmed desorption (TPD). This nominally simple UHV technique provides in principle a *direct, microscopic probe* of the complex interactions occurring on these well-defined organic materials.[6] As we will demonstrate, there exist in our experiments certain microscopic analogies to macroscopic wetting. We will further establish the short-ranged nature of the molecular interactions on these surfaces and illustrate the importance of steric screening effects in determining the interfacial properties of dense molecular solids.

A preliminary account of this work has recently been presented.[7] The current paper describes a significant elaboration of both the experimental program and highly qualitative correlations described in that earlier communication. In this work, we reexamine the qualitative interpretations given earlier, quantitatively treating the data where feasible, and recast our description of the data in the formalisms rigorously applicable to the interpretation of desorption kinetics. In so doing, we will present evidence which suggests a significant structural sensitivity of water desorption kinetics in what we infer to be microscopically wetted and nonwetted systems. These features will be correlated with the nature of the molecular architecture of the underlying substrate.

Experimental Section

Experiments were performed in a diffusion and titanium-sublimation-pumped UHV chamber with a base pressure of less than 1×10^{-10} Torr. The system was equipped with four-grid, low-energy electron diffraction (LEED) optics (Varian), a single-pass cylindrical mirror analyzer (PHI) for Auger electron spectroscopy (AES), and a differentially pumped quadrupole mass spectrometer (Vacuum Generators) for temperature-programmed desorption. The heating rate (β) was 1.0 K/s, except where noted otherwise in the text.

A 1-cm diameter Au(111) single-crystal disk (>99.99% pure), obtained from Cornell Materials Research Laboratory, was used as the substrate. The sample was oriented ($\pm 1/2°$), cut, and polished with use of standard metallographic techniques. It was then mounted on a small, temperature-controlled molybdenum block which was mounted in turn on a rotatable liquid nitrogen reservoir. The sample could be heated to over 1200 K by a tungsten filament inside the molbydenum stage or cooled to less than 90 K. Sample temperatures were measured by using a chromel–alumel thermocouple inserted *into* the gold substrate. The absolute temperature was calibrated by placing the sample in liquid nitrogen (77 K), dry ice/acetone (195 K), and ice/water (273 K) baths and is accurate to ±2 K. The crystal was cleaned of trace carbon, sulfur, and calcium impurities by repeated cycles of neon ion bombardment (1000 eV, 10–12 $\mu A/cm^2$) at both 300 and 900 K followed by annealing in vacuum at 900 K to restore surface order. Sample cleanliness and order were carefully monitored by using AES and LEED, respectively.

After the gold surface was cleaned, the vacuum system was brought up to atmospheric pressure with dry nitrogen, and the substrate was removed and placed in an ~0.001 M ethanol solution of the appropriate thiol ($HS(CH_2)_{15}X$: $X = CH_3$, CO_2CH_3, CO_2H, $CONH_2$). The syntheses of these adsorbates have been described previously.[1] After standing overnight at room temperature, the sample was removed from the solution, washed with copious amounts of fresh ethanol, and returned to the vacuum system. In several cases, the wetting properties of the samples were tested prior to their insertion into the vacuum chamber. Due to concerns about thermal effects on the structure of the monolayer, the chamber was not baked during the pump down. Experiments were begun when the background pressure (>75% H_2O) reached 1×10^{-9} Torr. In addition to the normal pumping present on this chamber, three internal liquid nitrogen traps were cooled in order to bring the pressure of the system to below 5×10^{-10} Torr during all TPD runs. Gas dosing was performed by using a calibrated, pressure-controlled, effusive molecular beam source. The exposures are given in units of langmuirs (1 langmuir = 10^{-6} Torr s). In those cases where a coverage is cited, this was calculated from the exposure assuming a unity sticking coefficient. Since all of the monolayers examined are extremely sensitive to electron beams, LEED and Auger studies were undertaken only after all of the adsorption experiments were completed.

In most water adsorption experiments, D_2O was substituted for H_2O because of the lower background intensity at $m/e = 20$ (control experiments indicated the absence of measurable kinetic isotope effects in these systems).

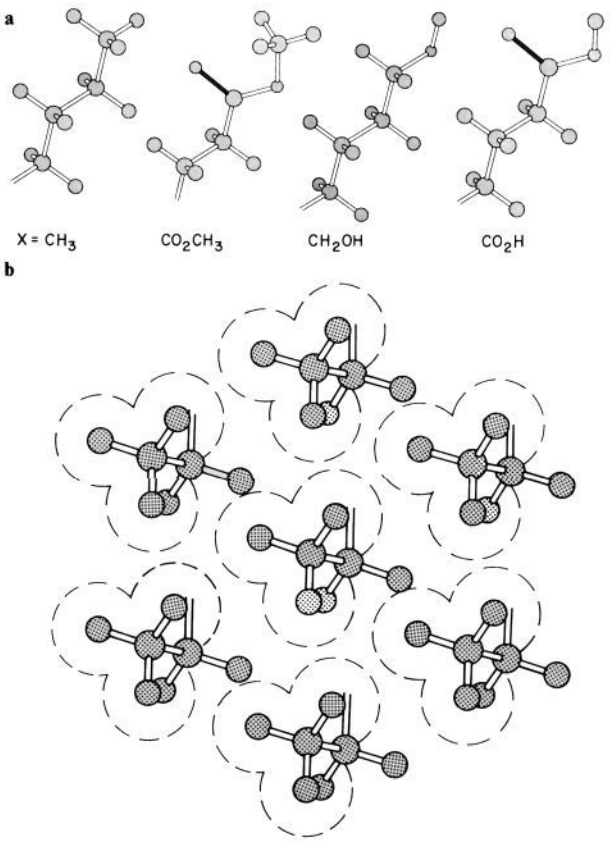

Figure 1. (a) Ball and stick projections (side) of the molecular orientations of representative monolayer adsorbates on gold. (b) Idealized surface projection of the methyl surface of a hexadecanethiol monolayer assuming a ($\sqrt{3} \times \sqrt{3}$) overlayer of sulfur atoms on the Au(111) lattice plane.[8] Only the last two carbon atoms of the monolayer are shown for reasons of clarity with the open circles approximately depicting the space-filling projection of the methyl group.

Results

General Remarks and Observations. The structures of the various adsorbate films on Au(111) employed in this study have been described in detail elsewhere.[1] In Figure 1 we present schematic representations of the molecular structures of several examples as the issue of conformational variations in the organic substrate is central to the subject of this paper. We will also, for convenience, refer to a specific monolayer film according to its terminal functional group. A hexadecanethiol film thus will be called a methyl surface, while that derived from 16-mercaptohexadecanoic acid will be referred to as the acid surface. The names of the others will follow similarly.

In Figure 1a are shown approximate side projections of the alkyl chains and head groups of the four derivatives whose structures were reasonably well-established by quantitative infrared spectroscopy[1] (as viewed from the side along the *y*-axis with the appropriate rotation and tilting of the trans zigzag chain occurring along the *z*-axis and *xz*-plane, respectively). The amide derivative is not shown since, as has been noted earlier,[1] there exists considerable uncertainty as to the orientation of this particular headgroup (the alkyl chain orientation is well-defined; however, we believe the structure of this derivative corresponds closely to that of the acid.). The projections shown of the other terminal functional groups are those which best conform with the IR data and with space-filling models packed so as to minimize steric interactions; a $\sqrt{3}$ interchain spacing,[8] as defined by the Au(111) lattice constant, was assumed in this latter model. Figure 1b shows

(6) See, for example: Madix, R. J. *Catal. Rev.* **1984**, *26*, 281–297 and references cited therein.

(7) Dubois, L. H.; Zegarski, B. R.; Nuzzo, R. G. *Proc. Natl. Acad. Sci. U.S.A.* **1987**, *84*, 4739–4742.

(8) (a) Electron diffraction: (TEM) Strong, L.; Whitesides, G. M. *Langmuir* **1988**, *4*, 546–558. (LEED) Dubois, L. H.; Nuzzo, R. G. Manuscript in preparation. (b) Helium diffraction: Chidsey, C. E. D.; Liu, G.-Y.; Rowntree, P.; Scoles, G. *J. Chem. Phys.* **1989**, *91*, 4421–4423.

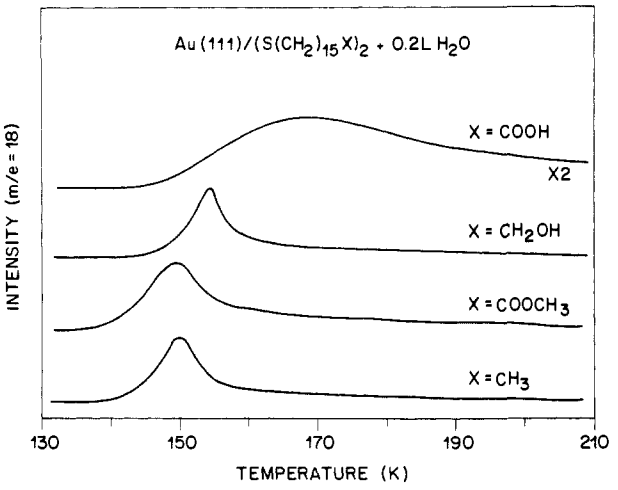

Figure 2. Survey TPD data for water adsorption on four monolayer substrates prepared from the adsorption of the indicated disulfides on Au(111). The water exposure used was 0.2 L in each in conjunction with a linear temperature ramp rate of 2.5 K/s.

a view of one representative surface, the "methyl surface" of a *n*-hexadecanethiol monolayer. The pseudohexagonal packing of the methyl groups is a highly idealized version of this surface. The notion of a hexagonal projection of the underlying alkyl lattice is one that is supported by both diffraction[8] and infrared data[1] as well as molecular dynamics calculations performed on a closely related model monolayer phase.[9] The figure makes one obvious suggestion about the nature of these films, namely that they form highly corrugated yet dense surface phases. It is also clear that the combination of the specific preferred headgroup orientations and the dense chain packing combine to present the chain-terminating functionality in a unique molecular environment, one which has little analogy in either solution-phase or solid-state chemistry.

In the preceding paper, we suggested that the dense packing of the headgroups that exists in these films could give rise to steric screening effects; that is to say that only a portion of the functional group will be accessible to molecules in a contacting phase. This effect and the relative sensitivity of TPD in studying molecular interactions of the sort of interest to this study are clearly demonstrated by the data shown in Figure 2.[10] This figure shows a qualitative survey of water adsorption on four different monolayer films: the methyl, methyl ester, alcohol, and carboxylic acid surfaces. The exposure in each case corresponds to ~20% of a geometric monolayer (assuming a near unity sticking coefficient, a reasonable assumption given the low surface temperature). It is evident that the interaction of water with the substrate is strongest on the carboxylic acid surface, a substrate capable of forming interlayer hydrogen bonds, and weakest on the two different methyl bearing surfaces. A comparison of the data for the two polar surfaces also suggests that the interaction with water is stronger on the acid surface than it is on the alcohol.[11] It is also evident that the polar groups of the ester, residing only a few angstroms from the surface, have little effect on the TPD profile inasmuch as the spectra strongly resemble those obtained with an aliphatic monolayer substrate. This result adds further credence to the idea that these surfaces are densely packed. It should also

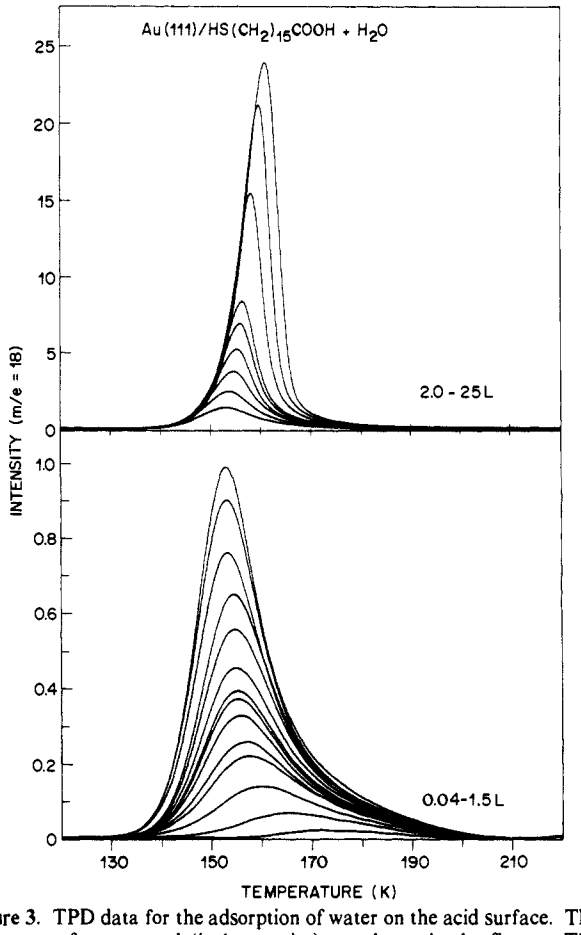

Figure 3. TPD data for the adsorption of water on the acid surface. The exposures of water used (in langmuirs) are shown in the figure. The temperature ramp rate was 1.0 K/s. The upper frame of the figure shows representative data obtained in the high exposure limit.

Table I. Wetting Properties of Organic Surfaces

surface termination/ adsorbate	T_m[a], K	E_a[b], kcal/ mol	ΔH_{sub}[c], kcal/ mol	contact angle, θ	zero-order onset, ML
acid/					
water	172.6	10.8	11.8	0–10°	~1
methanol	182.3	11.4	12.8	0°	~1
n-hexane	145.7	9.2	11.8	0°	~1
methyl/					
water	135.1	8.4	12.0	110°	<1[d]
methanol	135.7	8.4	12.4	22°	~1
n-hexane	131.3	8.1	11.8	0°	>1
amide/					
water	148.3	9.2	11.2	0–10°	≲1
methanol	157.5	9.8	11.6	0°	~1
n-hexane	–	–	–	0°	–
ester/					
water	147[e]	8.9	–	95°	<1
alcohol/					
water	154[e]	9.4	–	0–10°	–

[a] Peak maximum measured for the lowest coverage experiment. [b] Calculated according to the method of Redhead[18] at the lowest coverage observable assuming $\nu = 1 \times 10^{13}$ s^{-1}. Specific interpretations are discussed in the text. [c] Determined from a zero-order rate analysis (eq (3)) of multilayer data obtained for exposures of the secondary adsorbate of ≥10 L. [d] Significant "undercutting" of TDS curves observed. [e] Data from Figure 2, heating rate = 2.5 K/s.

be noted that the TPD characteristics seen for water on the carboxylic acid surface, in terms of peak shape and coverage dependent shift of the maximum, appear to be generally indicative of strong interlayer hydrogen-bonded interactions (see Figure 3 and ref 7).

Simple correlations can be made between the data in Figure 2 and contact angle data, a macroscopic measure of adsorption

(9) Cardini, G.; Bareman, J. P.; Klein, M. L. *Chem. Phys. Lett.* **1988**, *145*, 493–498. Bareman, J. P.; Cardini, G.; Klein, M. L. *Phys. Rev. Lett.* **1988**, *60*, 2152–2155.

(10) These data were obtained with monolayer substrates derived from the corresponding disulfides. The structures of these films and their TPD properties are almost indistinguishable from those derived from thiols. See: ref 1, 7, and (a) Nuzzo, R. G.; Fusco, F. A.; Allara, D. L. *J. Am. Chem. Soc.* **1987**, *109*, 2358–2368. (b) Bain, C. D.; Troughton, E. B.; Tai, Y.-T.; Evall, J.; Whitesides, G. M.; Nuzzo, R. G. *J. Am. Chem. Soc.* **1989**, *111*, 321–335.

(11) Theoretical calculations suggest that the bond strengths for linear hydrogen bonds to water will be ~2.4 kcal/mol stronger for a carboxylic acid as compared to an alcohol. These results compare well to the qualitative trends established by TPD. See: Schuster, P. In *The Hydrogen Bond*; Schuster, P., Zundel, G., Sandorfy, C., Eds.; North-Holland: New York, 1976; pp 109–110.

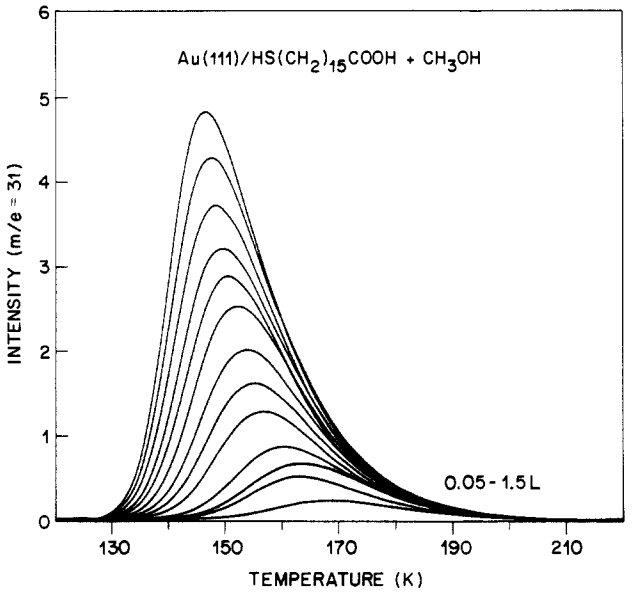

Figure 4. TPD data for the adsorption of methanol on the acid surface. The exposures of methanol used are shown in the figure. The temperature ramp rate was 1.0 K/s. Note the tailing to high temperatures similar to that seen in the lower panel of the previous figure.

properties. Table I lists a compilation of this latter data as well as the results of TPD experiments described immediately below. It is clear that the lowest angle for water ($\theta \simeq 0°$ on the carboxylic acid surface) is observed on the surface for which TPD suggests the strongest interaction. For the very hydrophobic methyl surface ($\theta \simeq 110°$), TPD data suggest a weaker interaction. However, it is also clear, when one examines the data, that *such correlations* between TPD and contact angle data *are neither precise nor invariant*. This is easily seen by comparing the results for the acid and alcohol surfaces in Figure 2 and Table I. Contact angle data for water differ only slightly for these two polar surfaces; both are wetted. The temperature-programmed desorption data, however, are very different; indeed by this measure, it would seem that the alcohol and the methyl surfaces have similar adsorptivities for water. It thus follows that *the two techniques measure different aspects of the relevant interfacial thermodynamics*. Even with this significant distinction, the qualitative notions derived from macroscopic wetting studies remain instructive and provide useful models for the interpretation of TPD data. For example, the contact angle data for the specific adsorbate–substrate pairings listed in the table demonstrate a transition between completely wetted and nonwetted states. As we shall see later, these macroscopic phenomena have microscopic analogies.

We will now examine in detail the adsorption properties of several representative monolayer systems. In particular, our focus will be on those materials which our earlier study showed to have highly polar (carboxylic acid, 16-mercaptohexadecanoic acid), nonpolar (methyl, hexadecanethiol), and intermediate polarity (amide, 16-mercaptohexadecanamide) surfaces. By way of comparison, we will also describe the adsorption properties of the native Au(111) surface. The secondary adsorbates chosen for this study—water, methanol, and *n*-hexane—also represent a range of polarities and potential ability to interact strongly with either itself or the underlying substrate. We will discuss each surface in turn.

The Carboxylic Acid Surface. The TPD results for the adsorption of water, methanol, and *n*-hexane on this surface (Figures 3, 4, and 5, respectively) show a number of similar features. At the lowest coverages (<0.05 monolayer), the peaks are broad and asymmetrically skewed toward the high temperature side. The temperatures at which the peak maxima occur in the sub-monolayer regime are also found to decrease with increasing surface coverage. This latter effect is especially pronounced for the hydrogen-bonding adsorbates, water and methanol, and less so for *n*-hexane (an adsorbate which interacts through dispersion forces only).[12] At higher coverages, approaching and/or exceeding a monolayer of the adsorbate, a dramatic change in line shape occurs (see, for example, Figures 3 and 5). These latter line shapes (especially the leading edge which remains invariant with respect to the initial surface coverage) reflect the onset of simple zero-order desorption kinetics. Further comment on these points is deferred to the discussion section.

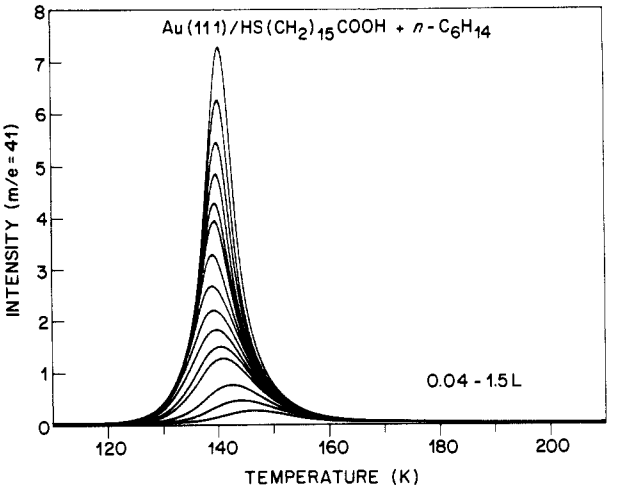

Figure 5. TPD data for the adsorption of *n*-hexane on the acid surface. The exposures of *n*-hexane used are shown in the figure. Similar data were recorded for *n*-hexane adsorption on the methyl surface. The temperature ramp rate was 1.0 K/s.

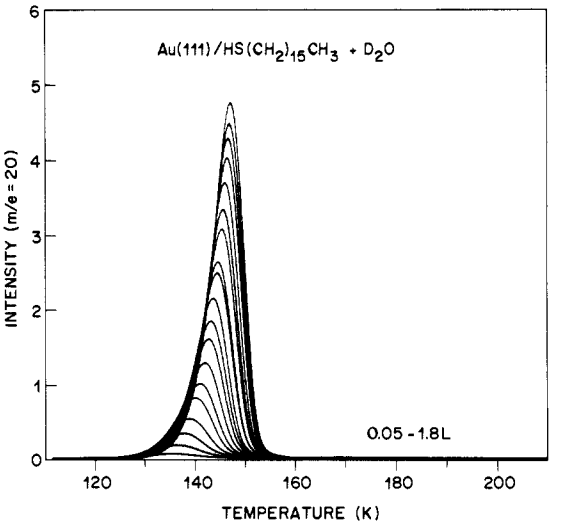

Figure 6. TPD data for the adsorption of deuterated water (D_2O) on the methyl surface. There was no significant kinetic isotope effect observed in these experiments. The exposures of water used are shown in the figure. The temperature ramp rate was 1.0 K/s.

The Methyl Surface. It is well-documented in the literature that the dense packing of methyl groups at a surface yields a film of low surface free energy.[2,10b,13] This characteristic property

(12) As was noted earlier, the background gases in the UHV chamber during these experiments are almost entirely water; the limited stability of the organic surface phases precluded our baking the apparatus. It is thus likely that some water condensed on the sample surface during the cool down cycle between TPD experiments. We are uncertain as to how large a quantity this might be (certainly <5% of a monolayer). How this influences the TPD results is unclear in a quantitative sense, although, qualitatively, it seems reasonable to expect that the measured values of ΔH_{sub} would be somewhat higher than the value for the pure phase. The results above suggest this effect is small; however, it also should be noted that this issue in no way precludes the examination of internal trends, especially as regards the influence of the various substrate phases on the TPD data.

(13) See, for example: Shafrin, E. G.; Zisman, W. A. *J. Colloid Sci.* **1952**, *7*, 166–182. Allara, D. L.; Nuzzo, R. G. *Langmuir* **1985**, *1*, 45–52 and references cited therein.

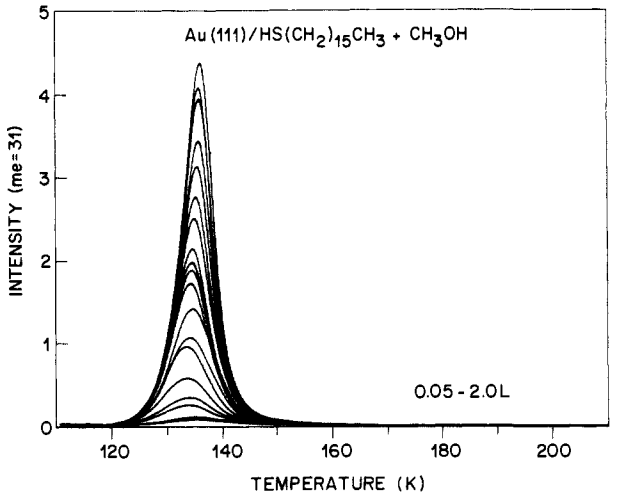

Figure 7. TPD data for the adsorption of methanol on the methyl surface. The exposures of methanol used are shown in the figure. Note that the zero-order desorption regime is reached at far less than monolayer coverage. The temperature ramp rate was 1.0 K/s.

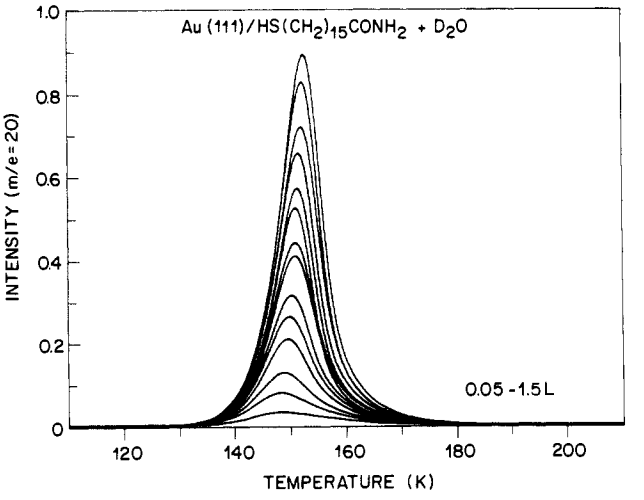

Figure 8. TPD data for the adsorption of deuterated water (D_2O) on the amide surface. The exposures of water used are shown in the figure. The temperature ramp rate was 1.0 K/s.

is evident in TPD data as well. Water, an adsorbate capable of forming strong intermolecular hydrogen bonds, exhibits a desorption profile which is completely different than that found on the more polar, hydrogen bond forming carboxylic acid surface. Figure 6 shows TPD data obtained over a range of coverages varying from a few percent of a monolayer to up to ~20 monolayers of water. Several features of the data deserve specific comment. First, the temperature of the peak maxima increases monotonically with coverage. Second, the peaks show apparent and significant undercutting across a considerable range of coverages. With the exception of this undercutting, whose origin is discussed later in the text, the desorption kinetics for this adsorbate–substrate pair can be described by invoking a simple zero-order rate regime *even at very low initial coverages of water.* The behavior with methanol, another hydrogen bond forming adsorbate, is shown in Figure 7. It is obvious that these latter spectra bear strong qualitative similarities to the water desorption data on this same surface. One significant difference is that we do not see undercutting of the leading edge of the desorption peak in this instance. The onset of the zero-order rate regime is found to occur, as was the case above, at extremely low coverages, on the order of a few percent of a monolayer. The hexane desorption data proved to be unexceptional (strongly resembling those shown in Figure 3 and ref 7) and are not shown here.

The Amide Surface. Our earlier studies suggested that this surface is of intermediate polarity—that is the TPD behavior falls between the extremes defined by the acid and methyl surfaces—with regard to the microscopic adsorption properties of water. This result is somewhat surprising in view of the well-known strong hydrophilicity and hydrogen-bonding affinity the amide group possesses in solution-phase environments. The contact angle data shown in Table I do not shed much light on this point. It is clear from the water contact angle data that the amide surface is far more polar than the methyl derivative. How it differs from the acid is unclear as they are both sufficiently polar to be completely wet by water. The TPD data shown in Figures 8 and 9 illustrate that wetting, at the microscopic level at least, is of a very different character on this surface than it is on the acid substrate. The water data (Figure 8) show some indication of *a strong water–substrate interaction at the very lowest coverages.* As the initial coverage of water increases beyond ~10% of a monolayer, the data seem to indicate that the nature of the desorption kinetics has changed. The peak temperatures, which had initially decreased with coverage, now begin to increase markedly until, at ~1 monolayer of water, the onset of zero-order desorption kinetics is clearly observed.

The behavior of methanol (Figure 9) is also very different on this surface as compared to the others discussed above. As is clearly evident in the data shown in the figure, a higher temperature state is selectively populated at low coverage. This state shows a coverage dependence of the temperature at which the peak maxima occur which is reminiscent of but less extreme than that seen for methanol on the acid surface. As the coverage approaches a monolayer, a second state is observed, one characteristic of the multilayer.

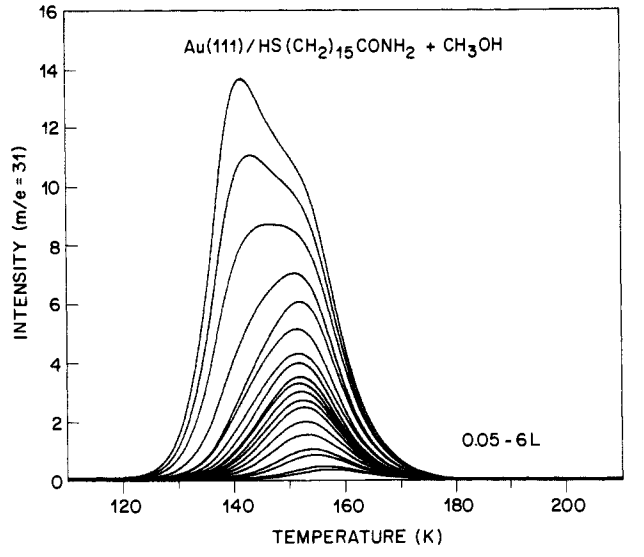

Figure 9. TPD data for the adsorption of methanol on the amide surface. The exposures of methanol used are shown in the figure. Monolayer and multilayer desorption features are clearly visible. The temperature ramp rate was 1.0 K/s.

Finally, we note that, due to the close similarity evidenced by *n*-hexane on the two preceding substrates and in our previous studies,[7] we did not examine this adsorbate here.

The Clean Au(111) Surface. The adsorption of *n*-hexane, methanol, and water on a clean gold surface is characterized by properties which are for the most part quite different from that observed on any of the organic surfaces. A clear example of this is shown in Figure 10 which presents data for the adsorption of *n*-hexane on Au(111). The three main peaks observed are due to the desorption of *n*-hexane from a monolayer (210 K), bilayer (144 K), and multilayer (135 K), respectively. The monolayer peaks are described by first-order desorption kinetics, while that for the multilayers is of mixed character. Methanol also shows distinct monolayer, bilayer, and multilayer desorption from this surface although these three regimes are not as well-separated as they are for the case of *n*-hexane (see Figure 11). Water adsorption on this surface (Figure 12) is also quite distinct. The desorption kinetics we observe are first-order at the very lowest

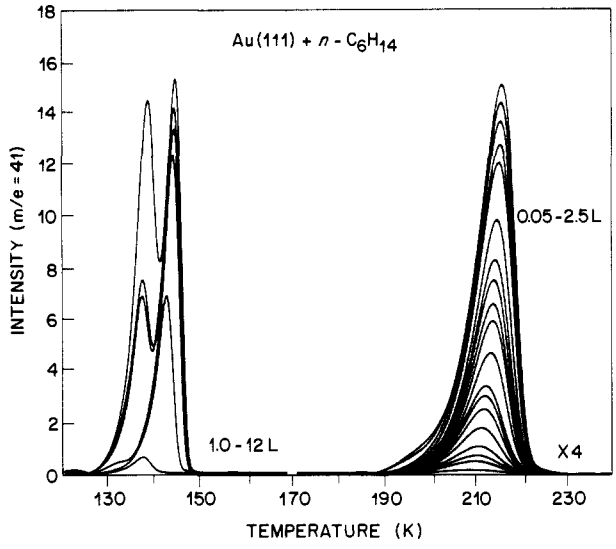

Figure 10. TPD data for the adsorption of *n*-hexane on the clean Au(111) surface. The exposures of *n*-hexane used are shown in the figure. The high coverage and low coverage data were recorded in two separate series of experiments. The temperature ramp rate was 1.0 K/s in both cases.

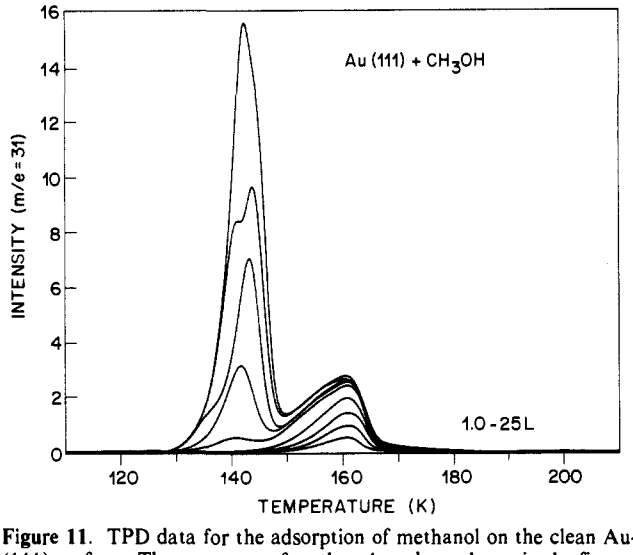

Figure 11. TPD data for the adsorption of methanol on the clean Au(111) surface. The exposures of methanol used are shown in the figure. Monolayer, bilayer, and multilayer features are clearly visible. The temperature ramp rate was 1.0 K/s.

coverages examined (a few percent of a monolayer) but rapidly switch to zero-order. This kinetic pattern is very similar to that described above for water adsorption on the methyl surface. The undercutting of each successive trace, so evident in the data recorded on the methyl-terminated surface, is not as pronounced here, however. The small, high temperature shoulder is presumed to be due to the desorption of water from defects.

Discussion

Analysis of TPD Data. In the discussion which follows we will attempt to relate the data presented above to those issues relevant in wetting. In particular, we will seek to correlate both the qualitative and quantitative aspects of TPD with the macroscopic behavior evidenced by contact angles. TPD is not calorimetry, however; it is a technique for measuring the *kinetics* of desorption. In the present instance, we are concerned with "simple" processes—that is to say desorption processes that break the fairly weak intermolecular interactions of organic species. In this very special case, where the desorption transition state is in essence the final, unbound state of the overlayer adsorbate molecule in vacuum, the activation energy we measure in TPD can be directly related to the heat of adsorption.

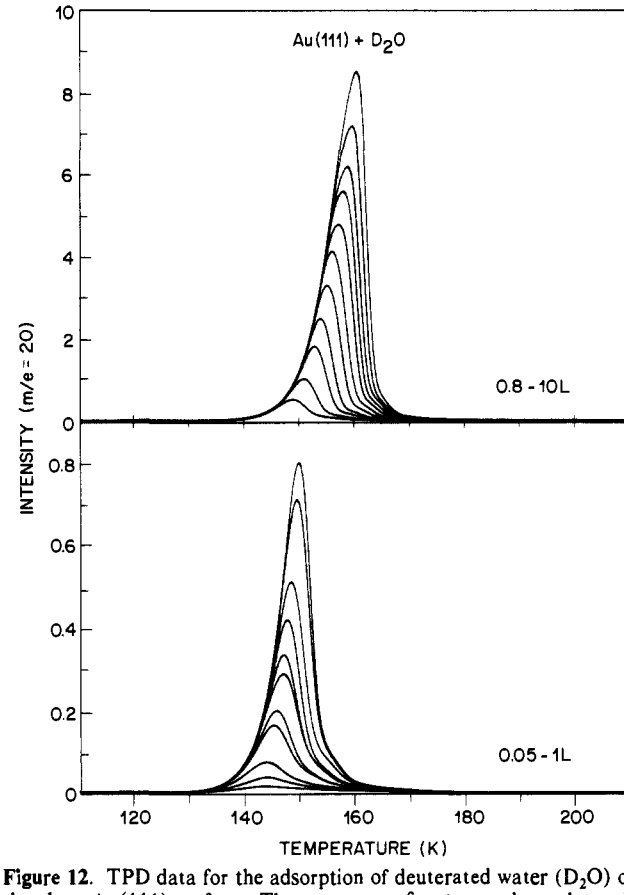

Figure 12. TPD data for the adsorption of deuterated water (D_2O) on the clean Au(111) surface. The exposures of water used are shown in the figure. The upper panel shows data obtained in the high exposure limit. In contrast to the previous two figures, only a single desorption feature is observed. The temperature ramp rate is 1.0 K/s.

Analysis of TPD data assumes that the desorption rate exhibits an Arrhenius-like dependence on temperature, as described in the following expression

$$I \sim \frac{-dn}{dt} = (n)^x \nu(n,T) e^{-\epsilon_a(n,T)/RT} \qquad (2)$$

where I, the intensity measured by the mass spectrometer, is proportional to dn/dt, the change in the surface coverage, n, as a function of time. The parameters ϵ_a and ν are the coverage- and temperature-dependent activation energy and preexponential factor for desorption, respectively. The reaction order, x, may also be coverage-dependent. Since the temperature range over which desorption occurs in these experiments is narrow, the weak temperature dependence of ν and ϵ_a can be safely ignored. In addition, we ignore any effects which might arise due to a temperature dependence in the structure and/or order of either the surface or the overlayer.[8b]

The one case we can interpret with considerable confidence is the desorption of molecules from a *multilayer* of the secondary adsorbate. This is done by deleting the surface coverage dependence in eq 2 ($x = 0$, $\nu(n) = \nu$, and $\epsilon_a(n) = \epsilon_a$). In this limit,

$$\ln(-dn/dt) = \ln \nu - \epsilon_a/RT \qquad (3)$$

Thus a plot of the log of the desorption intensity vs $1/T$ (when the data sets are suitably truncated, see below) yields ϵ_a directly. This value should be equal to the heat of sublimation (ΔH_{sub}) of that particular adsorbate.[14] The results of these analyses are

(14) Care must be taken in the analysis of the water data since the slow adsorption of water vapor onto a cold substrate yields amorphous solid water. This is a metastable species, however, and the transition to crystalline ice occurs between ~120 and 160 K depending on both the film thickness and the nature of the substrate. See, for example: Sceats, M. G.; Rice, S. A. In *Water: A Comprehensive Treatise*; Franks, F., Ed.; Plenum Press: New York, 1982; Vol. 7 and references cited therein.

shown in Table I. Inspection of the data indicates that the average values found for water, methanol, and *n*-hexane on the various surfaces agree well with literature values for the heats of sublimation (11.7 vs 11.5,[15] 12.1 vs 11.7,[16] and 11.8 vs 12.1[17] kcal/mol, respectively).

Interpretation of the data obtained at low coverages presents a number of significant challenges. First and foremost among these is deciding how to quantify the data. We have analyzed our spectra by using a number of techniques and find most of them to be unsuitable. Why do these standard methods fail? There appear to be several reasons. Careful inspection of the TPD data in the low coverage regime ($\lesssim$1 monolayer, especially Figures 3, 4, 6, and 7) reveals that the desorption traces do not display "classical" line shapes.[18,19] As we will show, this deviation from classical behavior reflects the *varying coverage dependences of* ν, ϵ_a, *and* x for a given adsorbate on that particular surface. As a result, techniques which make assumptions about the molecularity of the process or the dependence of ν and ϵ_a on n will not be suitable.[18-20] We have also found that "model independent" analyses,[21] which make *no* apriori assumptions about ν and ϵ_a, yielded results which were physically unreasonable (highly coverage dependent but very low values of ϵ_a). We are uncertain as to why these analyses fail but suspect the following factor as a prominent contributor. In low temperature desorption events of this sort, the peaks are narrow (of the order of 10–15 K), and, as a result, the change in the magnitude of the rate constant that is analyzed is too small to yield a reliable calculation of ϵ_a. "Differential" techniques, when used to analyze the leading edge of each desorption trace, were also found to yield unreliable results.[22] Finally, "order" plots (ln I vs ln n)[23] always show significant curvature, a clear indication that either the order of the desorption or the preexponential factor are coverage dependent.

Given that established analytical methods fail to treat the type of complex TPD data described in the figures correctly, there appears to be little justification to attempt an analysis more sophisticated than that given by Redhead.[18] With the *assumptions* of first-order desorption, a preexponential term of 1×10^{13} s^{-1}, and the use of the temperature of the peak maximum (T_m) from the lowest coverage experiment, values of ϵ_a—and thus the heat of adsorption—can be calculated. The results of this very simple analysis are shown in Table I. It is obvious that all of the numbers calculated in this manner are *too small*. For example, water on the acid surface, where the T_m's of the sub-monolayer data are actually at *higher* temperatures than that found for the multilayer, is calculated to have a heat of adsorption that is *at least 1 kcal/mol less* than that of the binding enthalpy of the multilayer. The principal source of the analytical failure in this instance is our assumption that $\nu \simeq 1 \times 10^{13}$ s^{-1} (a point we will return to later). Inspection of the "Redhead" result for water on the methyl surface also indicates that the analysis yields a nonphysical result. The error in this case, however, is much too large to be explainable by an incorrect choice of ν. The failure here reflects the inadequacy of the assumption that *the kinetics of desorption* on this substrate *can be described by a simple first-order rate law*.

Microscopic Clustering and Nonwetting. As we mentioned earlier in the Results section, the desorption of water from the methyl surface exhibits zero-order rate behavior at the onset to desorption, even at initial coverages of the adsorbate that are substantially less than one monolayer. The fact that the desorption processes are so different for water on the methyl and acid surfaces suggests a very significant feature relevant to the structure of water on these two materials. The simplest issue to address is what one intuitively expects for water on the methyl surface. We know from the contact angle data that this surface is extremely hydrophobic; indeed the values of θ for H_2O measured on these surfaces ($\sim$ 110–115°) are the highest known for an all aliphatic material.[10b] In simpler language, we say it is not "wetted" by water. In the UHV environment at these temperatures there seems little doubt that this adsorbate would diffuse laterally on the substrate and *cluster* with other water molecules. The self-interaction energy is simply too large and the activation energy of diffusion too small for it to be otherwise.[24] This clustering is conceptually a direct microscopic equivalent of the nonwetting seen in contact angle studies and is clearly observed via its influence on the nature of the desorption kinetics.[25,26] This is shown schematically. In this

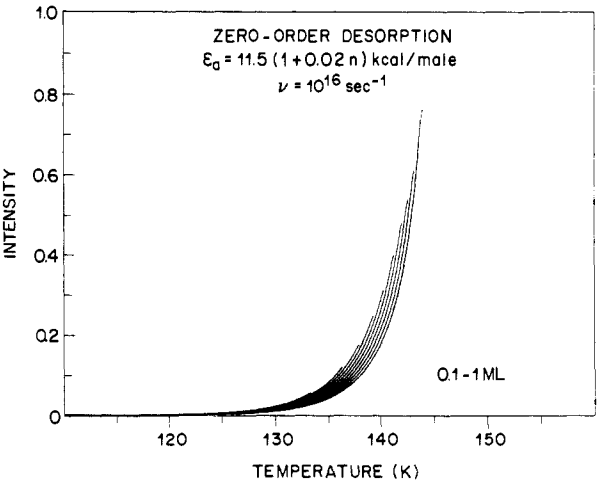

Figure 13. Desortion onsets calculated by using a zero-order rate dependence (eq 3) and a coverage-dependent ϵ_a (ϵ_a = 11.5 (1 + 0.02n) kcal/mol). The preexponential was fixed at 1×10^{16} s^{-1}, and the heating rate was assumed to be 1.0 K/s. The initial coverage was varied from 0.1 monolayer (ML, lower trace) to 1 ML (upper trace). The vertical scale is deceptive since the calculations performed here do not include a transition to a first-order rate regime.

Scheme III

$$A_{m(ads)} \underset{k_1}{\overset{k_{-1}}{\rightleftharpoons}} A_{m-1(ads)} + A_{(ads)} \xrightarrow{k_d} A_{m-1(ads)} + A_{(g)}$$

simplified model, m is a large number indicating that the A molecules are clustering into domains of unknown structure on the surface. By presuming that there exists a preequilibrium between A strongly bound in the cluster and less strongly bound on the substrate, the desorption process (k_d) will exhibit zero-order kinetics so long as the size of the cluster is sufficient to saturate this preequilibrium.[25,26] The simplest form of this kinetic model also involves the desorption of water as a monomer; this was found experimentally to be the case.[27]

As was mentioned earlier, the singularly most diagnostic feature indicating the presence of a zero-order rate regime is a rising edge of the TPD trace which is invariant with changes in the initial coverage of the adsorbate (that is to say x = 0 in eq 2). This

(15) Eisenberg, D.; Kauzmann, W. *The Structure and Properties of Water*; Oxford Press: New York, 1969.
(16) This value is estimated from the reported values of the heats of vaporization and fusion. See: Yaws, C. L. *Physical Properties, a Guide to the Physical, Thermodynamic and Transport Property Data of Industrially Important Chemical Compounds*; McGraw-Hill: New York, 1977.
(17) This value is calculated for *n*-hexane at 0 K. See: Shipman, L. L.; Burgess, A. W.; Scheraga, H. A. *J. Phys. Chem.* **1976**, *80*, 52–54.
(18) Redhead, P. A. *Vacuum* **1962**, *12*, 203–211.
(19) Chan, C.-M.; Aris, R.; Weinberg, W. H. *Appl. Surf. Sci.* **1978**, *1*, 360–376.
(20) Soler, J. M.; Garcia, N. *Surf. Sci.* **1983**, *124*, 563–570. Niemantsuerdiert, J. W.; Wandelt, K. *J. Vac. Sci. Technol.* **1988**, *A6*, 757–761.
(21) King, D. A. *Surf. Sci.* **1975**, *47*, 384–402. Bonczek, F.; Poppa, H.; Todd, G. *Surf. Sci.* **1975**, *53*, 87–109.
(22) Habenschaden, E.; Küppers, J. *Surf. Sci.* **1984**, *138*, L147–L150.
(23) Falconer, J. L.; Madix, R. J. *J. Catal.* **1977**, *48*, 262–268.
(24) Recent studies have shown that water can readily diffuse and cluster on copper and palladium surfaces at temperatures as low as 25 K. Nyberg, C.; Tengstal, C. G.; Uvdal, P.; Andersson, S. *J. Electron. Spectrosc. Relat. Phemom.* **1986**, *38*, 299–307.
(25) Arthur, J. R. *Surf. Sci.* **1973**, *38*, 394–412. McCarty, J. G.; Madix, R. J. *Surf. Sci.* **1976**, *54*, 210–228.
(26) Nagai, K.; Hirashima, A. *Appl. Surf. Sci.* **1988**, *33/34*, 335–341 and references cited therein.
(27) We have observed gas-phase dimers in the desorption of formic acid from a methyl surface, however. Some dimer desorption is expected here given the strength of the hydrogen bonding in this system.

appears to be the case for methanol on the methyl surface (where $\theta > 20°$) for a considerable range of coverages less than a monolayer. This behavior is especially pronounced for water on Au(111) and, with the exception of the noted undercutting, on the methyl surface as well (where $\theta \simeq 60°$ and 110°, respectively).

The undercutting seen in water desorption from the methyl surface does not imply that our assumption about the desorption rate order is wrong. We feel that the coverage dependence in this case is expressed in the exponential term of eq 2 (i.e., the binding enthalpy is coverage dependent). Figure 13 shows a plot of a calculated zero-order rate regime (from eq 3) in which the activation energy has been allowed to vary by 2% of the limiting value as a linear function of the coverage. The input parameters are $\epsilon_a \simeq 11.5$ kcal/mol (the average binding enthalpy derived from the zero-order rate analysis of the multilayer data, see above) and $\nu \simeq 1 \times 10^{16}$ s^{-1}. The high preexponential factor is consistent with desorption from a "constrained" adsorbate and has been seen for other strongly hydrogen-bonded systems on weakly interacting substrates.[25] It is clear that the curves both reasonably match the leading edge onsets seen experimentally and undercut with changes in the initial coverage in the appropriate manner. Why, one might ask, is this physically reasonable? It is well-known that there exist in water both strong, short-ranged nearest neighbor interactions and less strong, yet significant, long-range dipolar interactions (varying with distance as r^{-3}). It is well-established that these latter forces (which are, in fact, stabilizing) give rise to a strong size dependence of the binding enthalpy of water in gas-phase clusters.[28] We feel that the undercutting seen in Figure 6 is a clear indication of this same effect occurring for water clusters adsorbed on a surface. This is a *very subtle effect*, however, and should be sensitive to the sizes of the clusters present on the surface. The differences we note between water on the methyl surface and Au(111) (in terms of undercutting) presumably reflect differences in the nucleation and hence sizes and structures of the clusters present on these two surfaces.[14,29] Empirical calculations tend to support this latter point.

Adsorbate Wetting. The arguments above seem to address reasonably those cases where the substrate is not "wetted" by the adsorbate. It is also clear that the other adsorbate–substrate pairs exhibit very different TPD profiles. The perturbations are especially pronounced in the pairings with low or zero contact angles, in particular those which are capable of forming strong, interlayer hydrogen bonds (especially water and methanol on the acid surface). Taking the acid surface as a representative example, the low coverage data suggest that the interactions of the adsorbates with the substrate are sufficiently strong so as to preclude clustering of the adsorbates into large islands. In these more two-dimensional phases, the kinetics of desorption at coverages less than a monolayer are likely to be described by a first-order rate law. Let us consider the specific case of the acid surface first.

Inspection of the data shown in Figures 3, 4, and 5 suggests that the interactions with the substrate are strong; we can reasonably infer this from the fact that the low coverage peaks are shifted to significantly higher temperatures than those derived from higher substrate coverages. Both water and methanol show strong asymmetries to the high temperature side and very distinct dependences of the line shapes and peak maxima on the initial coverage. These peak shifts are much more pronounced for methanol as one might expect intuitively. It is also clear from an analysis of the peak shapes that the desorption of methanol and water from the acid surface exhibits coverage-dependent kinetics, even in the sub-monolayer regime, which cannot be explained by a *simple* rate law in which either ϵ_a or ν are invariant with coverage. In order to understand the origin of this coverage dependence, it is useful to do an analysis which *presumes* simple first-order kinetics and a preexponential factor of 1×10^{13} s^{-1} (see Table I). Although this is certainly wrong in detail, it does provide

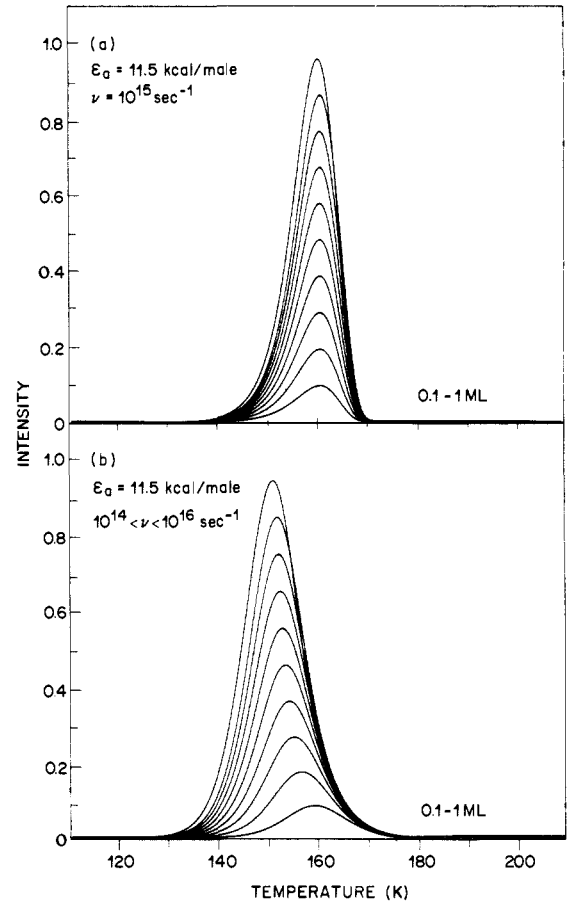

Figure 14. Desorption traces calculated by numerically integrating eq 2 with a constant activation energy (ϵ_a = 11.5 kcal/mol) and assuming either (a) $\nu = 1 \times 10^{15}$ s^{-1} or (b) ν varies linearly from 1×10^{14} to 1×10^{16} s^{-1} as the coverage increases from 0 to 1 monolayer. The heating rate was assumed to be 1.0 K/s in both cases.

instructive information. It is clear that the assumptions inherent in this analysis *do not* lead to the determination of correct values for ϵ_a. It is thus obvious that, irrespective of the correct order of the kinetics, the proper preexponential factors for the desorption of water and methanol are significantly larger than 1×10^{13} s^{-1} and are, in all likelihood, coverage-dependent as well. Although we expect the coverage dependence of ν to be small (varying from $\sim 10^{14}$ s^{-1} at low coverage to $\sim 10^{16}$ s^{-1} at saturation), it nonetheless can explain successfully both the coverage dependent shift in T_m and the high temperature tailing observed in all of the spectra of Figures 3 and 4.

A qualitative representation of these trends is illustrated by the analysis of a model water desorption experiment shown in Figure 14. These plots were obtained by numerically integrating eq 2 with a constant activation energy (again assuming that $\epsilon_a = 11.5$ kcal/mol) and $x = 1$. In (a), $\nu = 1 \times 10^{15}$ s^{-1}, while in (b) ν varies linearly with the coverage, n, from $\sim 1 \times 10^{14}$ to 1×10^{16} s^{-1}. This figure hows how profoundly the line shape changes from the classical form (shown in the upper panel) when ν is coverage-dependent. The sign of this effect suggests that a more "ordered" initial state is formed as the surface coverage increases. This also seems consistent with qualitative notions of the properties of lateral hydrogen bond forming systems.[25]

It is important to note that these discussions should only be taken as qualitative descriptions of what we feel are the important, broader trends evidenced in the data. Our kinetic models are too poor[30] and the data too complex to allow rigorous quantitation

(28) Suck Salk, S. H.; Lutrus, C. K. *J. Chem. Phys.* **1987**, *87*, 636–642.
(29) An extensive discussion of water adsorption on metal, semiconductor, and insulator surfaces is presented in: Thiel, P. A.; Madey, T. E. *Surf. Sci. Rep.* **1987**, *7*, 211–385.

(30) We have, for example, neglected the influence strain due to adsorbate–substrate misfit. Such strain can lead to Stranski–Krastanov film growth (i.e., uniform monolayer formation followed by 3-dimensional island growth) even in systems which exhibit strong substrate–adsorbate interactions. Grabow, M. H.; Gilmer, G. H. *Surf. Sci.* **1988**, *194*, 333–346.

of the relevant interfacial thermodynamics with use of TPD alone. In the case of the wetting interactions of water on the acid surface discussed immediately above, there exists at least one conceptually attractive alternative to the kinetic model we proposed. If we assume that the surface is heterogeneous in some manner, the data may simply reflect the unresolved desorption processes associated with these multiple-binding states. In a kinetic model, this effect would be expressed as a coverage-dependent activation energy. We have explicitly modeled this process and find that, in general, our earlier calculations assuming a coverage-dependent preexponential factor give a more reasonable approximation to the observed line shapes. Compensating effects between ϵ_a and ν may certainly be masked in the data,[20] and a rigorous analysis must take explicit account of such an occurrence. Molecular beam and infrared studies currently in progress in our and other laboratories may eventually shed light on this intriguing issue. We must stress, however, that any heterogeneity on these surfaces must be of a molecular scale.[31]

The amide surface demonstrates some interesting properties which merit explicit mention. The TPD data for water clearly indicate that its interaction is weaker than that on the acid surface ($\Delta(\Delta H) > 1$ kcal/mol at the lowest coverages assuming equal preexponential factors, see Table I). This is quite surprising in that it is well-known that the amide moiety is enormously hydrophilic, much more so than a carboxylic acid in its protonated form. It is assumed that much of this property reflects the greater basicity of the carbonyl oxygen in this functional group relative to a carboxylic acid.[32] Thus, there must exist in these substrate phases some structural aspect not found in typical solution enviornments which results in the inverted water affinities observed experimentally. We can hypothesize on several possibilities. The first of these we have considered is the influence of substrate intermolecular hydogen bonds (those formed *within* the acid or amide surface layers) on the binding potential of water. If we assume that any strong interaction with water would require the prior "breaking" of bonded pairs in the substrate and further given that these anhydrous "dimer" bonds should be stronger for an amide, one can completely rationalize the observations presented above. There exists, however, some spectroscopic evidence which weakens the credibility of one key assumption in this interpretation. Our IR data for the free substrate surfaces indicate that the intermolecular hydrogen-bonding interactions in the amide may be weak.[1] In fact, the only suggestion of a strong, interlayer pairwise interaction was found for the acid, whose nonsolvated structure is believed to be a dimer. This spectroscopic data would thus appear to be at odds with any simple model of the sort mentioned above. There is, however, one fairly simple way in which molecular orientations can contribute to the properties we observe. The preceding paper in this series presents evidence that the amide moiety is highly oriented in this assembly; the projection of the carbonyl group is believed to be largely *lateral into the neighboring molecules in the layer* resulting in the primary exposure of the NH_2 group at the interface.[1] This arrangement should partially screen the CO group from the interfacial environment, consistent with the perturbed properties measured by TPD.

The results for methanol are also instructive and provide a suggestion that there is a range of complex behavior observable at the low temperatures of the TPD experiment that have no explicit analogy in contact angle studies. In this system, it is clear that a specific adsorption state exists which is preferentially filled prior to the observation of the characteristic multilayer state. Our analysis suggests that this state is stabilized by ~0.8 kcal/mol relative ot the multilayer. It seems likely that this adsorbed state must involve significant hydrogen bonding to the N-H bond of the amide.

The clean Au(111) surface exhibits a range of behavior in TPD experiments with these adsorbates. Several specific features of this data merit comment. It is clear, for example, that the interaction between gold and hydrocarbons is strong (see Figure 10). Were it not for the dominant Au-S interaction,[1,33] the ~2.0 kcal/mol of aliphatic CH_n group bonding would preclude the molecular orientations which characterize these monolayers. A similar result (i.e., the occurrence of a strongly bound monolayer state) is obtained for methanol. Both the latter species show the formation of bilayer and multilayer states (clearly indicating "wetting" behavior). The TPD results for water have been discussed earlier. As was noted then, the zero-order desorption kinetics seen even at very low coverages of water compels one to assume the occurrence of adsorbate clustering on this substrate.[24]

Finally, we note that all of the various adsorbates studied can exhibit coverage-driven transitions between rate regimes (for example, zero- to first-order). This is strongly suggested by order plots and is one of the major reasons why quantitative interpretation of the data is so difficult. Where this transition occurs for each adsorbate-substrate pair remains an important and still unresolved question. It is particularly significant for water adsorption given the importance of aqueous interfaces in biological systems. There exists in our data some suggestion that this transition can occur, even on strongly interacting substrates (i.e., the amide and perhaps, although less likely, the acid surface), at coverages of less than a monolayer. The curvature observed in desorption order plots indicates that this is not an abrupt transition but, rather, a gradual one. Given the complex character of these data, we cannot offer any definitive analyses of this. More refined, albeit experimentally complex, approaches will be required to establish precisely when and how these coverage-driven transtions occur.[34]

TPD vs Contact Angle. We make one last comparison between our TPD data and the results of contact angle experiments. Figure 2 presented a survey of water desorption spectra from four surfaces. There exists in this data a striking similarity between the TPD profiles of water on the methyl and ester surfaces. The contact angle data in Table I also show these surfaces to be hydrophobic. In this sense, then, both experiments yield similar observations. There is, however, a difference between the contact angles measure on these two monolayers. We can calculate, by using standard methods, the differences in the work of adhesion on these surfaces and, by equating this difference solely to an interfacial enthalpy, estimate an apparent difference in the expected heat of adsorption; this value is judged to be ~0.8 kcal/mol.[2] We can calculate a zero-order water desorption onset (appropriate in this coverage range for these substrates—see above) using this enthalpy difference and compare that to the data in Figure 2. We find that, were the contact angle data to be predictive, the desorption onsets should be shifted by at least 15 K for these two surfaces. This is clearly not seen. It seems likely that this is a reflection of the differing "phase states" which exist in the two experiments. *In TPD, the relevant binding enthalpy that bounds the "wetting" transition is the heat of sublimation.*

(31) This picture is strongly supported by the extensive wetting studies which have been performed on these and other materials (see ref 3-5 and 10b and citations given therein), including ones in which impurities have been deliberately introduced into the film structure. The IR studies (see ref 1) which we have performed also demand that whatever surface reconstructions exist must be consistent with a largely crystalline polymethylene lattice projection. It is also clear that, at low temperature, the number of gauche conformations (necessary to populate any extensive reconstruction of the surface) must be exceedingly low. Indeed, recent He diffraction studies have demonstrated that the methyl surfaces of *n*-alkyl thiol monolayers are ordered at 100 K.[8b] It would thus seem that, to whatever extent the acid surface is viewed as being heterogeneous, that this property is *intrinsic* to a dense carboxylic acid surface phase.

(32) For example, the approximate pK_a values of

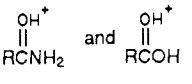

relative to water are −1 and −6, respectively. See: March, J. *Advanced Organic Chemistry: Reactions, Mechanisms, and Structure*; McGraw-Hill: New York, 1968; pp 219-220.

(33) Nuzzo, R. G.; Zegarski, B. R.; Dubois, L. H. *J. Am. Chem. Soc.* **1987**, *109*, 733-740.

(34) One potential approach is suggested by studies of xenon adsorption on tungsten. See: Opila, R.; Gomer, R. *Surf. Sci.* **1981**, *112*, 1-22. Alternatively, molecular beam surface scattering may be required.

Thus there exists a direct correlation with contact angle data only for those cases where $\theta \simeq 0°$ and where the heat of immersion is of the order of ΔH_{sub}.[35] We can now see why the zero-order desorption onsets discussed above are unshifted. In both cases the minimum in the potential surfaces is that due to the water–water rather than the water–substrate interaction. It is not possible, in such instances, to probe these latter states directly with TPD.

Using these simple notions, it is apparent that the water-binding properties of the three polar surfaces (acid, amide, and alcohol) can be classified with regard to which potential dominates the TPD data; for the acid and amide it is clearly that due to the substrate–water interactions, while for the alcohol it is that due to the self-interaction of water. These latter insights also implicitly establish a structure-property correlation that would not be evident in a contact angle study (since $\theta \simeq 0°$ for each), namely the relative affinities of these surfaces for water: acid $\gtrsim$ amide > alcohol. This suggests but one of the potential advantages which result from a consideration of data from both types of measurements. Even so, we advise caution in making extrapolations from one to the other. For example, it seems reasonable that there may exist surface reconstructions in these systems which might have an important bearing on interfacial properties in the temperature ranges appropriate to contact angle and solution phase reactivity studies; at the low temperatures used in TPD (necessary to operate in UHV) these same states might not be accessible.[8b,9]

(35) This does not take account of the complexities which might arise as a result of the temperature dependence of any of the relevant thermodynamic parameters, however.

Concluding Remarks

Our data suggest that certain conceptual analogies exist between contact angle behaviors (which measure macroscopic adsorption properties) and TPD profiles of microscopic UHV adsorption properties on these molecular surfaces. The desorption kinetics are complex in all instances and suggest that coverage dependences other than that related to simple mass action principles need to be considered. We present evidence that long-range dipolar interactions are important for at least water overlayers and that these interactions are, in fact, stabilizing.

Future papers will present additional examples of interfacial studies of such model organic solids as well as apply vibrational spectroscopy to the task of resolving several of the issues related to the complex molecular environments which exists at these interfaces and the structures formed by various overlayers.

Acknowledgment. We thank J. C. Tully for several illuminating discussions on the analysis of TPD data. We are also grateful to Professor G. Whitesides and his co-workers for their critical evaluation of an early draft of this manuscript. C. E. D. Chidsey and G. Scoles and his co-workers are also gratefully acknowledged for their communication of results prior to publication.

Through-Bond and Through-Space Interactions in a Series of Cyclic Polyenes

M. F. Falcetta,[†] K. D. Jordan,*[,†] J. E. McMurry,[‡] and Michael N. Paddon-Row*[,§]

Contribution from the Department of Chemistry, University of Pittsburgh, Pittsburgh, Pennsylvania 15260, Department of Chemistry, Cornell University, Ithaca, New York 14853, and School of Chemistry, University of New South Wales, P.O. Box 1, Kensington, New South Wales, 2033 Australia. *Received February 21, 1989*

Abstract: Electron transmission spectroscopy is used to determine the electron affinities of tetracyclo[8.2.2.2^{2,5}.2^{6,9}]-1,5,9-octadecatriene and pentacyclo[12.2.2.2^{2,5}.2^{6,9}.2^{10,13}]-1,5,9,13-tetracosatetraene. The electron transmission measurements indicate that the splittings between the π^* anion states of these compounds are at most a few tenths of an electronvolt. It is shown, with the assistance of ab initio molecular orbital calculations, that both through-bond (TB) and through-space (TS) interactions between the π^* (and π) orbitals of the above compounds and of tricyclo[4.2.2.2^{2,5}]-1,5-dodecadiene are sizable but that these two interactions oppose one another causing the net splittings in the π^* EA's and πIP's to be small. A simple perturbation molecular orbital model is presented which accounts for the trends in the IP's and EA's. Molecular orbital calculations are carried out which show that if the ethano bridges separating the ethylenic groups are replaced by trimethylene bridges, then the balance between the TB and TS effects is altered, and the splittings in the π^* and π manifolds are increased.

I. Introduction

The nature of the intramolecular interactions between functional groups in polyatomic molecules is a problem of fundamental importance. In the nomenclature of Hoffmann et al. such interactions may be classified as either through-space (TS) or through-bond (TB).[1] The former is a direct interaction and falls off rapidly with increasing separation between the groups. The latter involves a coupling through the connecting σ-bond framework and generally falls off slowly with the number of σ-bonds separating the functional groups.[1-3] In an orbital model, the net coupling between equivalent functional groups is associated with the splittings between the relevant molecular orbitals (MO's).

In the present study the interactions among the ethylenic π and π^* orbitals of tricyclo[4.2.2.2^{2,5}]-1,5-dodecadiene (**1**), tetracy-

[†] University of Pittsburgh.
[‡] Cornell University.
[§] University of New South Wales.

(1) Hoffmann, R.; Imamura, A.; Hehre, W. J. *J. Am. Chem. Soc.* **1968**, *90*, 1499. Hoffmann, R. *Acct. Chem. Res.* **1971**, *4*, 1. Gleiter, R. *Angew. Chem., Int. Ed. Engl.* **1974**, *13*, 696. Paddon-Row, M. N. *Acc. Chem. Res.* **1982**, *15*, 245.

(2) Balaji, V.; Ng, L.; Jordan, K. D.; Paddon-Row, M. N.; Patney, H. K. *J. Am. Chem. Soc.* **1987**, *109*, 6957. Paddon-Row, M. N.; Jordan, K. D. In *Molecular Structure and Energetics*; Liebman, J., Greenberg, A., Eds., 1988; Vol. 6, Chapter 3, p 115.

(3) Many researchers have concluded that through-bond interactions fall off exponentially with the number of bonds separating the chromophores. (See for example: Paddon-Row, M. N.; Cotsaris, E.; Patney, H. K. *Tetrahedron* **1981**, *42*, 1779.) Other functional forms for the dependence of these interactions with the number of bonds have been suggested. (For a recent review: Mikkelsen, K. V.; Ratner, M. A. *Chem. Rev.* **1987**, *87*, 113.) However, there is agreement on the key point that through-bond interactions generally fall off much more slowly with distance than do through-space interactions.

0002-7863/90/1512-579$02.50/0